Industrial Crops & Products 141 (2019) 111750

Contents lists available at ScienceDirect

Industrial Crops & Products

journal homepage: www.elsevier.com/locate/indcrop

Mechanical activation and characterization of micronized cellulose particles from pulp fiber

Lang Huang[a,b,d], Qiong Wu[b,*], Qingwen Wang[c], Michael Wolcott[a,*]

[a] Composite Material and Engineering Center, Washington State University, 2001 East Grimes Way, Pullman, WA, 99164, USA
[b] Cultivation base of state key laboratory of ecological chemical industry, College of Chemical Engineering, Qingdao University of Science and Technology, 53 Zhengzhou Road, Qingdao, Shandong Province, 266042, China
[c] College of Materials and Energy, South China Agricultural University, 483 Wushan Road, Guangzhou, 510642, China
[d] Qingdao Institute of Bioenergy and Bioprocess Technology, Chinese Academy of Sciences, 189 Songling Road, Qingdao, 266101, China

ARTICLE INFO

Keywords:
Ball milling
Pulp fiber
Particle size and distribution
Crystallinity
Specific surface area

ABSTRACT

Ball milling has been widely used for cellulosic fiber pulverization and de-crystallization, but most of the previous milling studies are focused on the micro-structural change and crystallinity reduction of cellulose, few of them have evaluated the systematic influence of milling conditions and the energy efficiency. The objective of the study is to investigate and understand the effect of various ball milling parameters on the pulp fiber grinding performance. Ball mill time, rotational speed, charge ratio, mill ball diameters, and initial moisture content of pulp fiber were studied systematically from planetary ball milling. The pulverized particle size, particle morphology, crystallinity change, bonding disruption, thermal stability, specific surface area, and energy efficiency were evaluated during the milling process. Results revealed that cellulose fiber was mainly pulverized during the early milling stage (~20 min) and different variables led to changes regarding to the final particle size and shape. After refinement, the crystallinity and the thermal stability of the pulp fiber decreased, from the weakening or disintegration of the inter and intra hydrogen bonds of the cellulose chains. The specific surface area increased by 4~5 times with the particle size reduction, while the milling energy efficiency decreased after 40 min of milling time.

1. Introduction

As a low-cost, abundant and practical alternative source to substitute petroleum-based products, the cellulosic material is gaining increasing popularity for coping with the global environmental and energy-related issues. Various functionalized cellulose based materials has been widely applied in foods, chemicals, fuels, paper, clothing, cosmetics and bio-composites (Edgar et al., 2001; Klemm et al., 2006). Cellulose pulp fibers present great potential serving as reinforcing agent for polymer composite, especially attractive for those auto-manufacturers with eco-sustainable strategies to increase the bio-content in their products (Ashori, 2008; Balat, 2011; Bhatnagar and Sain, 2005; Siró and Plackett, 2010; Wu et al., 2007). However, the hydrophilic nature of commercially available cellulose fibrils are highly crystallized and tend to aggregate after pulping, bleaching and subsequent drying (Hult et al., 2001), which make it difficult to feed and disperse during the melt processing. In addition, the incompatibility interfacial adhesion and the high moisture sensitivity of cellulosic fibers make cellulose fibers reinforced composites limited for high value applications.

Cellulose is composed of D-anhydroglucopyranose unit (AGU) linked by 1,4-β-glycosidic bonds. Each AGU has three hydroxy groups located at C-2, C-3, and C-6 position, which are potentially capable for a variety of chemical reactions (Klemm et al., 2004). However, due to the large molecular mass, abundant intra/inter-molecular interactions (mainly hydrogen bonds), and highly organized fibrous structure, the reactivity of cellulose depends strongly on the accessibility of the hydroxyl groups (Kennedy et al., 1985). Different pretreatment procedures have been developed to weaken the interconnections and decrease crystallinity to increase the accessibility of cellulose, namely cellulose activation. The most common and easiest way to activate cellulose is loosening the cellulose supramolecular complex by breaking or reducing the interchain hydrogen bonds with swelling agents, such as DMSO (dimethyl sulfoxide) and DMF (*N,N*-dimethyl formamide), but the use of such agents appears to be increasingly unsustainable since they are hazardous, non-eco-friendly, and energy-demanding for the related solvent production, purification and recycling (Fidale et al.,

* Corresponding authors.
E-mail addresses: wuqiong0506@hotmail.com (Q. Wu), wolcott@wsu.edu (M. Wolcott).

https://doi.org/10.1016/j.indcrop.2019.111750
Received 2 January 2019; Received in revised form 28 June 2019; Accepted 31 August 2019
Available online 12 September 2019
0926-6690/

2008; Stone and Scallan, 1968; Thuresson et al., 1997).

Recently, significant effort has been made to develop environmental friendly procedures for cellulose treatments. Physical cellulose activating approaches, such as ball milling, which alter the cellulose supramolecular structure by breaking or reducing the interchain hydrogen bonds, are receiving increasing attention for their solvent-free, low cost advantages. Cellulose fibers subjected to ball milling not only results in disintegration at the macroscopic level, but also destroy the fibrillar architecture and reduce the crystallinity. In addition, grinding fibers into small particles leads to increased specific surface area and reduced defects in long fibers, which could be beneficial for subsequent treatments such as chemical reactions, sorption, or enzymolysis etc. Since Hess and co-workers (Hess et al., 1941) firstly disintegrated cellulose with a ball mill in 1941, ball milling has been widely empolyed on activating and modifying cellulsoe (Cellulose, 2010). Our previous studies investigated the microstructural changes of Douglas-fir from mechanical milling, revealing that ball milling was effective to break down the cell structure of wood fiber and promoted the bioconversion (Bon-Jae et al., 2019; Jiang et al., 2017; Liu et al., 2016). Ling et al. recently investigated the structure properties of the cotton fiber from ball milling using different techniques, indicating the amorphization of cotton fibers during milling (Ling et al., 2019). Even though various ball milling approaches offer promise in dealing with cellulosic fiber size reduction and crystallinity decrease, a deep understanding of the systematic influence of milling parameters as well as the energy efficiency is still lacking. During the milling process, the grinding inside the mill chamber is complex and strongly influenced by process parameters such as filling ratio, rotation speed, ball diameter etc., low energy efficiencies were reported for ore grinding using ball milling (Austin et al., 1976), while little information on analyzing the effect of ball milling parameters on the performance of ball milling cellulose was reported, except some study investigating the influence of the ball milling time factor. Therefore, it is vital to discern the influence of various milling parameters systematically and provide a guidance to operate ball mills under optimum conditions. In the study, faffy pulp fiber was subjected to planetary ball milling to prepare micronized cellulose particles, and the influence of milling conditions (i.e. ball milling time, filling ratio, rotation speed, ball diameter and cellulose moisture content) on the resulting particle size reduction, structure amorphization, thermal stability, specific surface area and energy efficiency was characterized and discussed. This work is intended to serve as a practical guide for subsequent laboratory studies, as well as industrial scale up applications for cellulosic material grinding.

2. Material and methods

2.1. Materials

In this study, pulp cellulose fiber used for milling was obtained from Weyerhaeuser Company (Federal Way, USA), stored in a conditional room at 20 ℃ and 65% relative humidity. Samples were subsequently conditioning to varied target moisture contents (MC) and validated using the gravimetric method. All the conditioned samples were stored in sealed plastic bags before use.

2.2. Milling machine and mill conditions

Mechanical milling was performed using a planetary ball mill (Across international, PQ-N04), with two 100-mL stainless steel jars and stainless balls. The ball milling time, rotational speed, ball to cellulose ratio, ball diameters and MC of the raw pulp materials were investigated using the single factor experiments described as following (Table 1), two replications were tested for each condition.

Table 1
Ball mill single factor effect study.

Sample sets	Ball milling time (min)	Ball to cellulose mass ratio	rotational speed (rpm)	Ball composition (mass ratio)	Moisture content (%)
1	10, 20, 30, 40, 50, 60, 90,120	60	600	ϕ10: ϕ6 = 1:2	3
2	30	30, 40, 50, 60, 70, 80	600	ϕ10: ϕ6 = 1:2	3
3	30	60	500, 530,560, 590, 620, 650	ϕ10: ϕ6 = 1:2	3
4*	30	60	600	all ϕ10, ϕ10: ϕ6 = 2:1, ϕ10: ϕ6 = 1:1, ϕ10: ϕ6 = 1:2, ϕ10: ϕ6 = 1:3, all ϕ6,	3
5	30	60	600	ϕ10: ϕ6 = 1:2	3, 6, 9, 12, 15

* Changing the composition of the balls but keep the total ball mass constant.

2.3. Particle size and distribution

The particle size and distribution of the milled cellulose fibers were evaluated by a laser scattering particle size analyzer (Malvern instrument, UK). Three parameters, d_{10}, d_{50} and d_{90} are recorded corresponding to the particle sizes of 10%, 50% and 90% percentiles from the cumulative size distribution, respectively. d_{50} is used to act as the average particle size and the dimensionless parameter Δd ($\Delta d = d_{90} - d_{10}$) is employed to represented the broadness of the particle size distribution.

2.4. Crystallinity study

An X-ray diffractometer (XRD, Rigaku, mini flex 600, Japan) equipped with a Cu kα ($\lambda = 0.154$ nm), radiated from 40 kV and 15 mA, was used to analyze the crystal structure of the ball milled cellulose powders. The 2θ ranges from 10 to 40°. The relative degree of crystalline, (*CrI*), can be obtained using the following equation (Segal et al., 1959).

$$CrI\ \% = [(I_{002} - I_{am}) / I_{002}] \times 100 \quad (1)$$

Where I_{002} is the intensity of the peak located around 22.6° and I_{am} refers to the minimum intensity between the main (22.6°) and secondary peaks (16.1°).

2.5. Morphology characterization

The particle morphology of the milled samples was studied by scanning electron microscopy (SEM, FEI Quanta 200 F, field emission gun ETD detectors, FEI Company, Oregon, USA). Cellulose particles were dried and then surface coated with gold before imaging. Pictures were taken at 20 kV accelerating voltage.

2.6. Thermal gravimetric analysis

Thermal gravimetric analysis (TGA) was conducted with a thermal analyzer (SDT Q600, TA Instruments) to assess the degradation temperatures. Cellulose samples approximately 10 mg in mass were heated from room temperature to 102 °C and held for 8 min. to evaporate the moisture content, then raised to 600 °C at a heating rate of 10 °C/min under a nitrogen atmosphere, with a purge gas flow of 100 μL/min.

2.7. FT-Raman analysis

Raman spectroscopy of cellulose powders was performanced on a Nicolet iS50 FT-IR spectrometer mounting a iS 50 Raman module accessory (Thermo scientific, USA). A single point defocused laser, powered at 0.4 W, was used for excitation. The spectra were collected from 250 to 3600 cm^{-1} at an average of 64 scans and a resolution of 4 cm^{-1}. All measurements were conducted at room temperature.

2.8. Cellulose specific surface area

Congo red dye adsorption (Inglesby and Zeronian, 2002) was used to measure the specific surface area of cellulose powder. First, Langmuir type adsorption of Congo red dye was prepared in 0.03 M phosphate buffer, with 1.4 mM NaCl and 1% cellulose substrate. Different dye concentrations (0.1, 0.2, 0.5, 1, 2, 3 g/L) were prepared and the samples were incubated at 60 °C and 180 rpm for 24 h. Then each suspension was centrifuged for 5 min. A UV–vis spectrophotometer (Lambda 25, Perkin Elmer) was employed to investigate the supernatant at a 498 nm wavelength. The maximum dye adsorption can be calculated using the following equation (Wiman et al., 2012):

$$\frac{[C]}{[A]} = \frac{1}{K_{ads}[A]_{max}} + \frac{[C]}{[A]_{max}} \quad (2)$$

Where $[A]$ (mg/g) refers to the dye adsorption by the substrate, $[C]$ (mg/mL) represents the free dye concentration, $[A]_{max}$ is the maximum dye amount adsorbed by cellulose powders (mg/g), and K_{ads} represents the adsorption equilibrium constant. The cellulose specific surface area (*SSA*) can be determined as shown below (Goodrich and Winter, 2007):

$$SSA = [A]_{max} \times N_A \times SA_{CR}/M_W \quad (3)$$

Here N_A refers to Avogadro's constant, 6.02×10^{23}; SA_{CR} represents the surface area for one Congo Red molecule, 1.73 nm^2; and M_W refers to the molecular weight of Congo red, 696.7 g/mol.

2.9. Energy consumption study

The milling energy consumption was investigated by a power logger (Fluke 1735, USA), and parameters including active energy, active power, frequency, time, and power factor were recorded. The specific milling energy consumption efficiency E_t (kJ/m^2) was calculated according to the following relation:

$$E_t = \frac{\int_0^t \Delta P_t\, d_t}{m(SSA_t - SSA_0)} \quad (4)$$

where ΔP_t is the power consumed at time t; m is the mass of pulverized pulp fiber (kg). SSA_0 and SSA_t are the specific surface area of the initial pulp fiber and t min ball milled sample, respectively.

2.10. Statistical analysis

The difference of the particle sizes of varied ball milling conditions were analyzed using the one-way Analysis of Variance (ANOVA) method employing R Commander software. A P-value less than 0.05 was considered statistically significant. Multiple comparisons between all pair-wise means were performed to determine how they differ.

3. Results and discussion

3.1. Ball milling time

In the planetary ball milling process, milling time is the most critical factor correlated to the overall input energy. Normally speaking, the ball mill energy input increased with the increase in operating time. The higher energy input allows for more collisions between the milling balls, filler materials and the chamber wall, leading to smaller and more uniform particles. As shown in Fig. 1, the ball milling time had a crucial influence on grinding the pulp fiber into small particles. After 10 min of ball milling, the long pulp fibers were ground into short fibers and the average diameter of the particles is approximately 130 μm, with a wide particle size distribution of $\Delta d = 467$. As the milling time increases, the input energy increased and the particles size continued to reduce. The average particle diameters for 20 min and 30 min are 103 μm, 69.3 μm, respectively. After 40 min ball milling, the average particle diameter decreased to 43.6 μm, with a $\Delta d = 82.2$. For further prolonging the ball milling, the particle size seems to reach a constant value and doesn't change too much, average diameters are 41.9 μm, 42 μm, 36.2 μm and 31.7 μm for 50 min, 60 min, 90 min and 120 min milling time, while the particle size distribution curve became narrower as milling time increased ($\Delta d = 86.1, 90.3, 70.4, 63.3$ for 50 min, 60 min, 90 min and 120 min milling). As shown in the Fig. 2, the Tukey confidence interval (CI) of the particle sizes for cellulose that has been ball milled for 50, 60 and 90 min are not significantly different from those of the 40 min milling times. That means that when the milling time reaches a specific value, the cellulose particles reached a critical size, and further grinding may not further reduce the final particle size. This result may have been limited by the design of the device and the milling ball diameters because when the cellulose particles reduced in size and reach a threshold value, it would require more energy than the effective milling collision

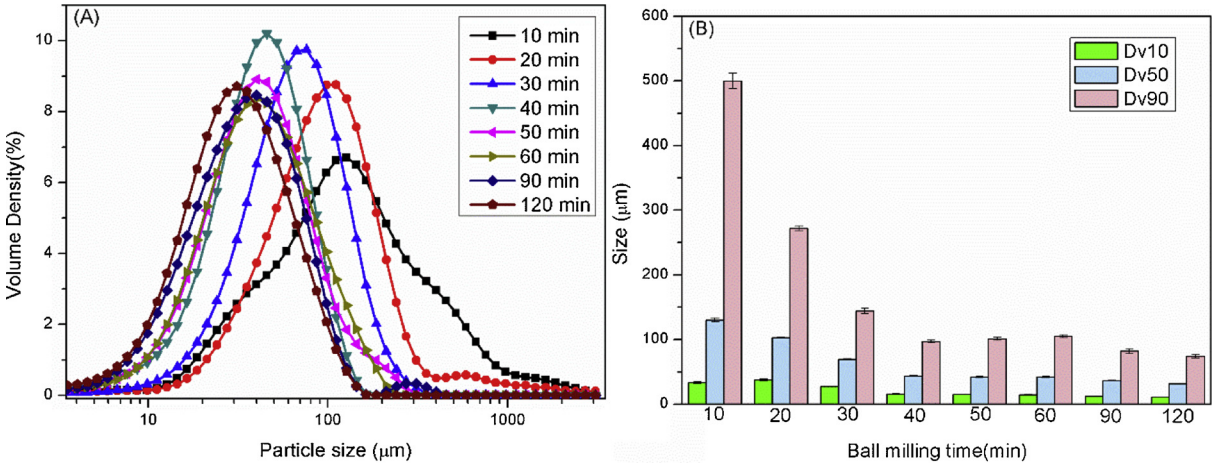

Fig. 1. (A) Volume based particle size distribution for varied mill time; (B) 10%, 50% and 90% percentiles particle sizes for different ball mill time.

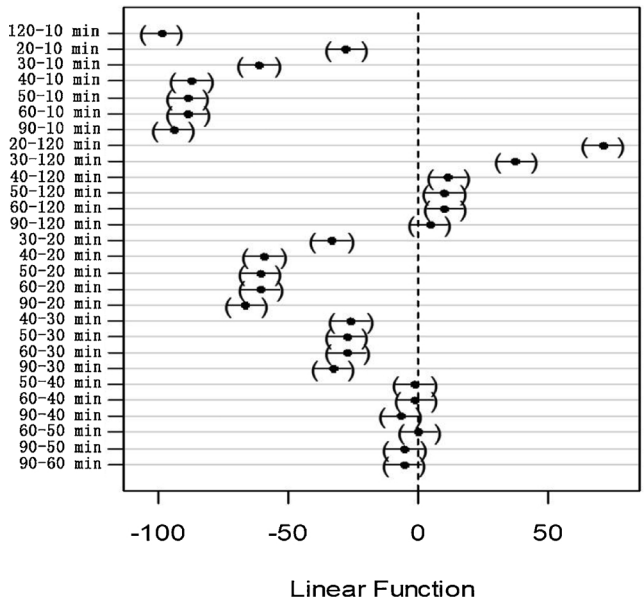

Fig. 2. Tukey simultaneous 95% CIs for different cellulose particles. Sample intervals that do not contain zero are significantly different.

could provide generating new surfaces.

3.2. Mass ratio of grinding media to feedstock

The grinding balls to feedstock mass ratio have long been an important variable for determining the milling efficiency. Mass ratios ranged from 1:1 to 200:1 have been previously used depending on the property of the charge materials and other milling conditions (Suryanarayana, 2001). In general, low bulk density material use a high mass ratio from the volume consideration. Fig. 3 demonstrated the effect of different milling mass ratios on the grinding behavior of the pulp fibers. Different ball to cellulose mass ratio of 30:1, 40:1, 50:1, 60:1, 70:1 and 80:1 were employed for investigating the grinding conditions shown in Table 1. These results illustrate that the ball to cellulose mass ratio significantly influences the resultant particle size of cellulose pulp fiber. At the ratio of 30:1, the milled particles showed a wide distribution (Δd = 638.4) and high average diameter (165 μm). As the ratio of ball to pulp fiber increased to 40, smaller (89.9 μm) and more uniform particles (Δd = 231) were achieved, but as the ratio increased to 50, large decreases in the diameter of the pulp particles were not found. The average particle diameters resulting from a ball to cellulose ratio of 50, 60, 70 were 71.9 μm, 69.5 μm, 59.1 μm, respectively. A higher ball to cellulose ratio increases the number of balls, which consequently increased the probability of ball-fiber collisions, increased the energy transferred to the cellulose, and led to more effective grinding. This trend could be demonstrated by comparing the particle sizes for the mass ratio of 30 with the higher ones. Too high pulp fibers fraction decreased the free space for the ball movement, leading to limited collision activities, while too low fiber concentration resulted in many invalid ball-ball or ball-chamber collisions and lowed the comminution efficiency. Therefore, the mass ratio of ball to cellulose should be controlled at 40 to 60 to get the most cost-effective performance.

3.3. Rotational speed

It is easy to realize that the higher rotation speed resulted in higher mechanical energy being applied to the milling materials, leading to better comminution. Rotational frequency encompasses the time factor and has a strong correlation to the rotational energy. The relationship between ball mill rotational speed and the resulting particle size was depicted in Fig. 4. When the rotational speed is 500 rpm, the milled cellulose powders had a larger average particle size and broader distribution compared to those of the higher rotational speed. The particle size decreased as the milling rotational speeding increasing. However, after 620 rpm, there is no significant difference in diameter for further increase of rotational speed. Every milling device has certain limitations for the maximum rotational speed based on the design. In the conventional planetary ball milling, speed increases the ball movement and raise the collision probability, leading to improved grinding, but above a critical rotational speed, the centrifugal forces will pin the balls to the inner chamber wall, which would lead to fewer collisions and decreased collisional energy (Suryanarayana, 2001). Therefore, it is essential to keep a moderate speed to maintain performance.

3.4. Ball diameter and combination

The diameter of the milling balls used in grinding is crucial for determining the final particle size and shape. The influence of adjusting the milling ball diameter and composition on the particles size was shown in Fig. 5. It can be seen that employing all large diameter balls resulted in an average particle size of 151 μm and Δd = 231, and all small balls led to an average particle size of 169 μm and Δd = 438. Large balls have a heavy mass resulting in high collision energy, however, since the overall mass is constant, the number of large balls is smaller than when small balls are included. This fact leads to fewer fiber-ball contacts. In contrast, small diameter balls have a larger number per unit mass and, therefore result in a high frequency of ball to

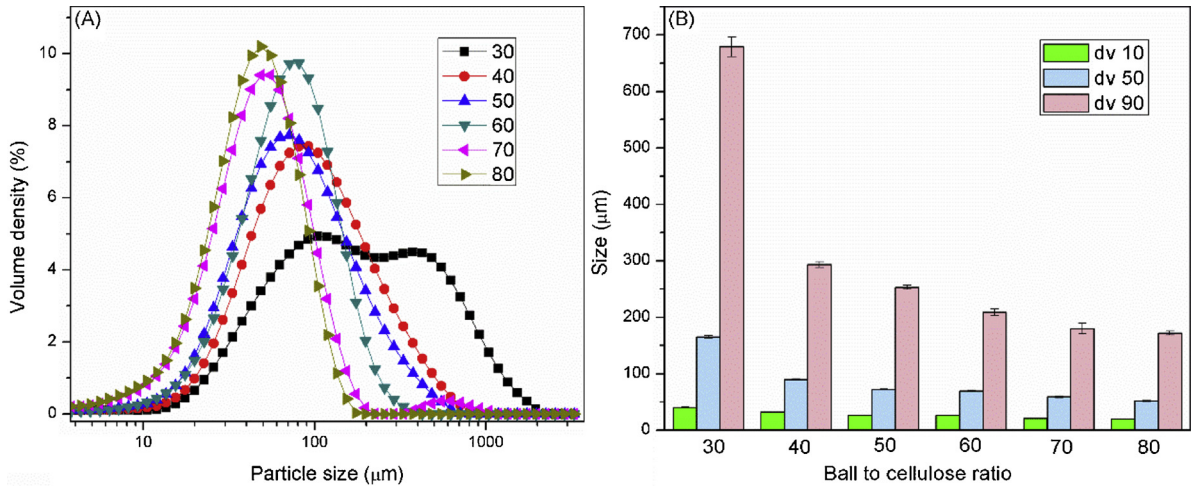

Fig. 3. (A) Volume based particle size distribution for varied ball to cellulose mass ratio; (B) 10%, 50% and 90% percentiles particle sizes for different ball to cellulose mass ratio.

cellulose collision but carry relatively low energy. This situation leads to difficulty in breaking the longer and stronger fibers, leading to a broad particle distribution. When combining different size balls, the particle size distribution curves shifted to low values. For example, at the mass ratio of the ϕ10 balls: ϕ6 balls = 1:2, the average diameter is 112 μm and Δd = 275. Different ball diameters with various speeds may have different movement routes and contact angles towards long fibers during the collisions. For the combination of different diameter balls, the larger balls are responsible for fracturing the long fiber into short ones, while the smaller balls increase the collision frequency and reduce the powder trapped between colliding bodies, grinding the powder into a more uniform shape and size. Therefore, a mixture of big balls and small ones, combined both advantages, resulted in a more effective grinding performance.

3.5. Moisture content

The initial moisture content of pulp fiber also affects the milling process. As shown in Fig. 6, the cellulose particles average diameters gradually increased as the initial moisture content changed from 3% to 15%. The average particle sizes and Δd for MC of 3%, 6%, 9%, 12% and 15% are, 41.9 μm and Δd = 86.1, 55.1 μm and Δd = 126.8, 63.3 μm and Δd = 149.9, 78.7 μm and Δd = 180.9, 86.5 μm and Δd = 193.4, respectively. For the milled cellulose pulp, the initial fiber moisture content affects the process in the following two ways: (1) the raw pulp material is a long fluffy fiber, when the MC below the fiber saturation point (approximately 30% for woody materials), the lower moisture contents lead to more brittle fiber behavior, which means lower moisture content pulp fiber is more easily fractured by the ball-fiber collision and results in smaller particles; (2) During the milling process, the moisture in the fiber can also act as a lubricant and decreases the collision energy between moving balls and fibers, slowing down the size-reducing process.

3.6. Morphology characterization

The SEM images for cellulose particles milled for 10 min, 20 min, 30 min, and 90 min were shown in Fig. 7. In the early milling stage (10 min), the initial long fibers were reduced into short fibers or high aspect ratio particles by the combined shear and impact forces, which might be produced by the large balls with high moving energy and resulting in rough surfaces and random shapes. As the milling time prolonging to 20 min, short fibers were continuously broken into smaller pieces, the aspect ratio reduced and the particles became ellipsoid in shape. After 30 min ball milling, more uniform cellulose particles were gained and the particle size decreased slightly, further increases the milling time to 90 min, part of the larger particles split into finer ones, and the particles are becoming more uniform in shape.

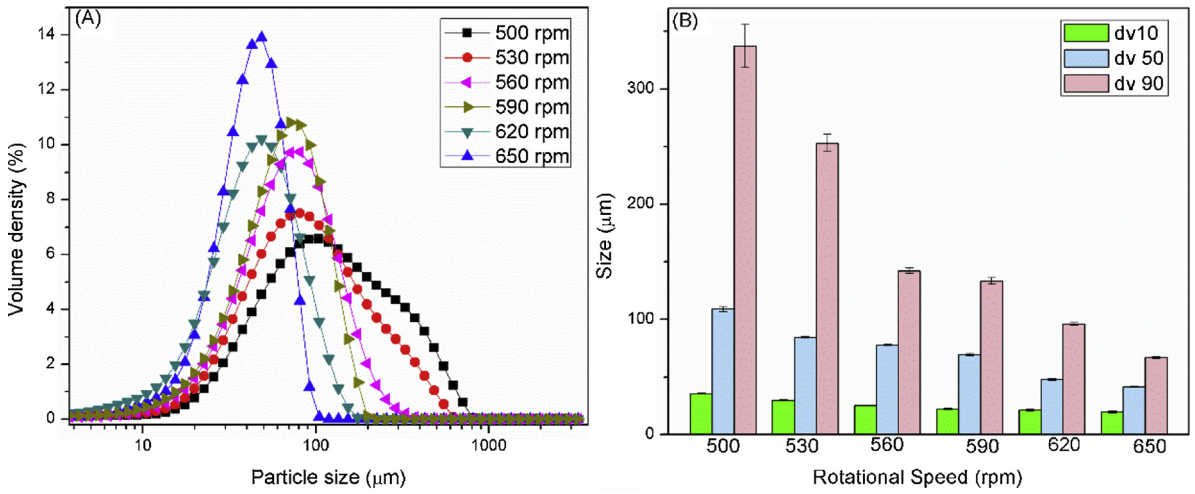

Fig. 4. (A) Volume based particle size distribution for varied rotational speed; (B) 10%, 50% and 90% percentiles particle sizes for different rotational speed.

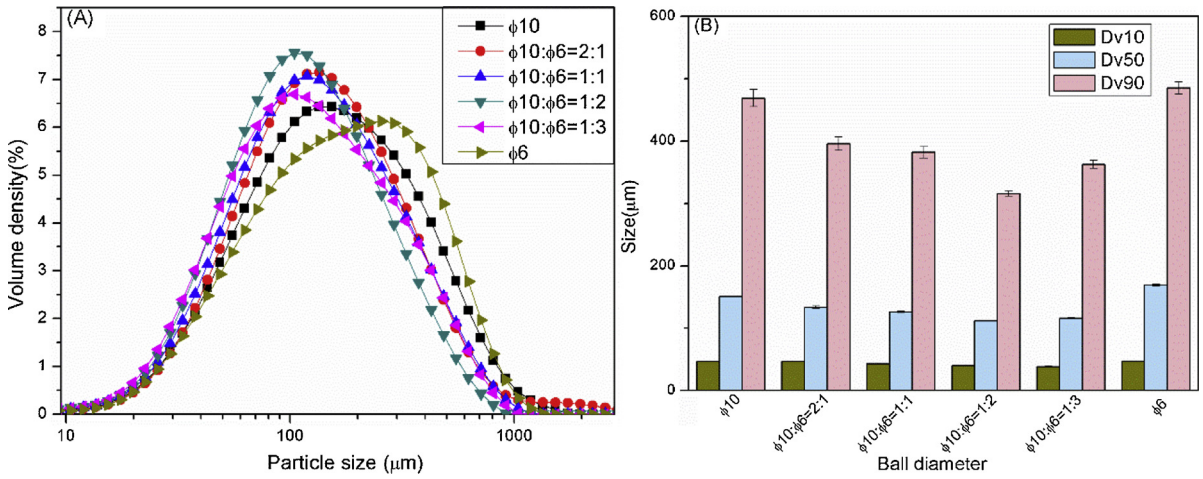

Fig. 5. (A) Volume based particle size distribution for different balls; (B) 10%, 50% and 90% percentiles particle sizes for different balls.

3.7. XRD analysis

Fig. 8 (A) exhibited the XRD curves for different time ball milled cellulose samples. For the pulp fiber sample before milling, two peaks appeared at around 2θ = 16.1° and 22.6° in the curve, related to the (101) and (002) diffraction planes from the cellulose crystalline structure, respectively (Isogai et al., 1989). As expected, the intensities of these two reflection peaks decreased with increased milling time. In the early milling stage, the two diffraction peaks signals decreased dramatically, supporting the notion that cellulose fibers were undergoing the de-crystallization process concurrent with size reduction. After 30 min of ball milling, the milled samples showed an announcement change in the XRD curve with the entire disappearance of the crystalline peaks at 2θ = 16.1° and 22.6° and replaced by the amorphous phase characteristic signal centered at approximately 2θ = 19.1°, which implies the highly ordered crystalline structure of cellulose was mostly destroyed and the amorphous phase resulted. Fig. 8 (B) presents the relationship between cellulose crystallinity and milling duration. The crystallinity of the raw material is 78.85%, and decreases dramatically with increasing ball milling time, ending with crystallinity of less than 20%. After 40 min of ball milling, most of the crystalline structure of the cellulose was eliminated and the amorphous particles resulted. Hydrogen bonds are responsible for most of the intra- and intermolecular interactions for the highly ordered, three-dimensional crystal structures, and the cellulose crystallinity has been directly related to the

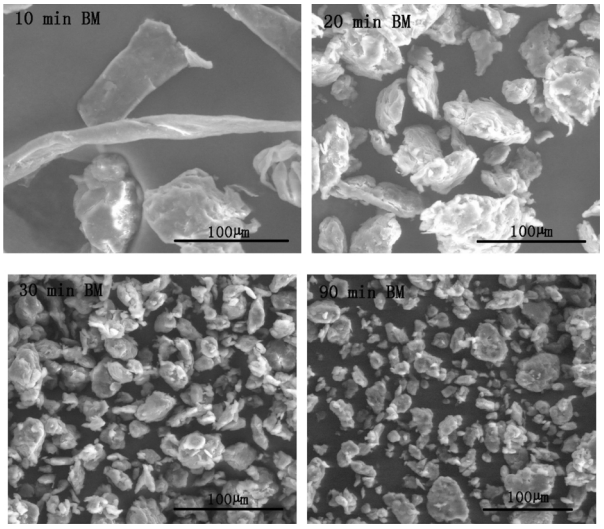

Fig. 7. SEM images for 10, 20, 30 and 90 min ball milled cellulose particles.

formation of these hydrogen bonds. During the ball milling process, as the long pulp fiber was broken down into micro-particles, the hydrogen bond based crystalline structure was also destroyed by the mechanical collisions, leading to the amorphous cellulose. After 40 min of milling,

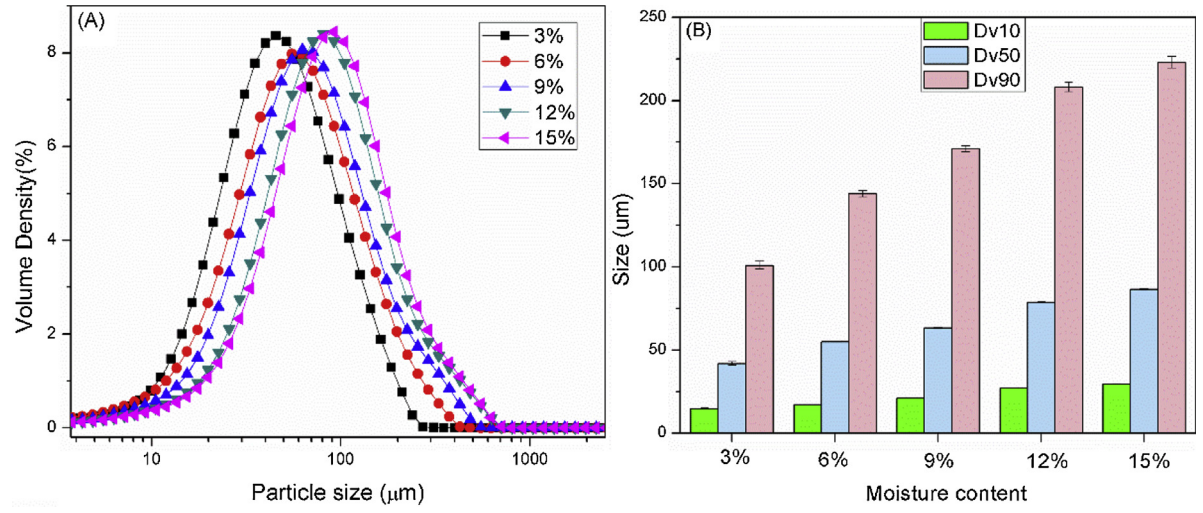

Fig. 6. (A) Volume based particle size distribution for different fiber MC; (B) 10%, 50% and 90% percentiles particle sizes for different fiber MC.

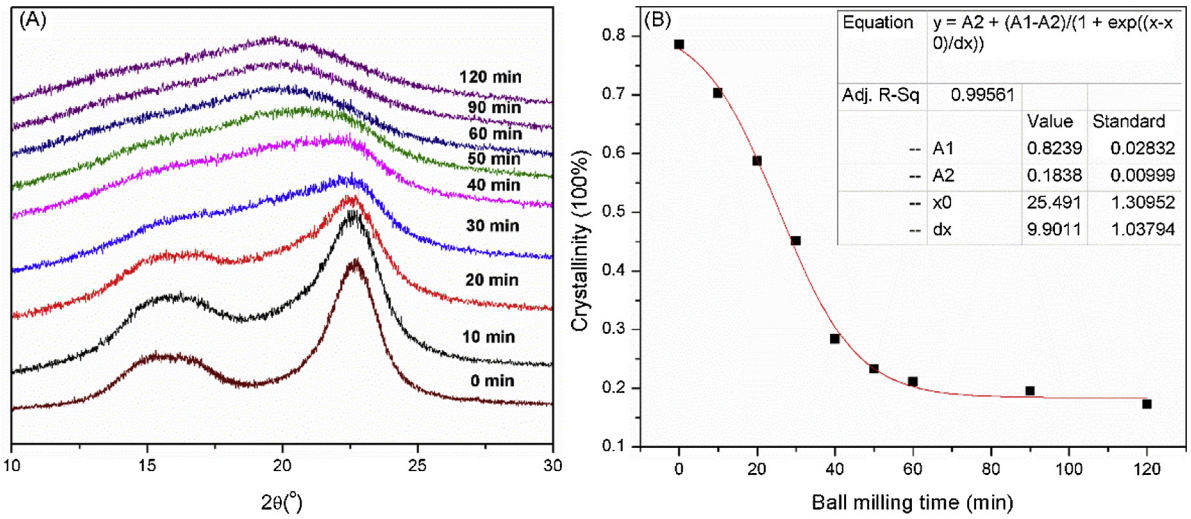

Fig. 8. (A) XRD curves for different time ball milled cellulose particles; (B) Crystallinity decrease fitting curve of cellulose particles ball milled for different time.

the particle size reached a threshold and a steady amorphous state equilibrium was attained.

3.8. Raman analysis

The structural difference of the cellulose powders following ball milling was also studied by FT-Raman analysis. The Raman spectra of the cellulose powders processed with varying milling times showed the most prominent changes in the fingerprint region. Fig. 9 presented the spectral changes in the range from 250 to 1700 cm^{-1} of the cellulose sample moving from crystalline state to the amorphous structure during milling. Peak 1095 and 1119 cm^{-1}, attributed to asymmetric and symmetric stretching for β-1,4 glycosidic linkage, respectively, could act as the monitors for the change in order of the cellulose structure (Edwards et al., 1997). The intensity of these two peaks decreased dramatically as the milling time increased, supporting the notion that fission of the interchain linkages occurred during the milling process. Peak 378 cm^{-1} and peak 1380 cm^{-1}, assigned to CCC ring bending and CH_2 modes, related to the crystallinity of the cellulose fibers (Alves et al., 2016), also weakened, suggesting that the de-crystallization process changes during the size reduction. After 30 min of balling milling, the spectra exhibited few changes for the 40, 50, 60, 90 and 120 min milling, which indicates that the de-crystallize process was mainly completed during the early milling stage and cellulose powders reached the equilibrium amorphous state after 40 min milling, as also supported by the XRD results above.

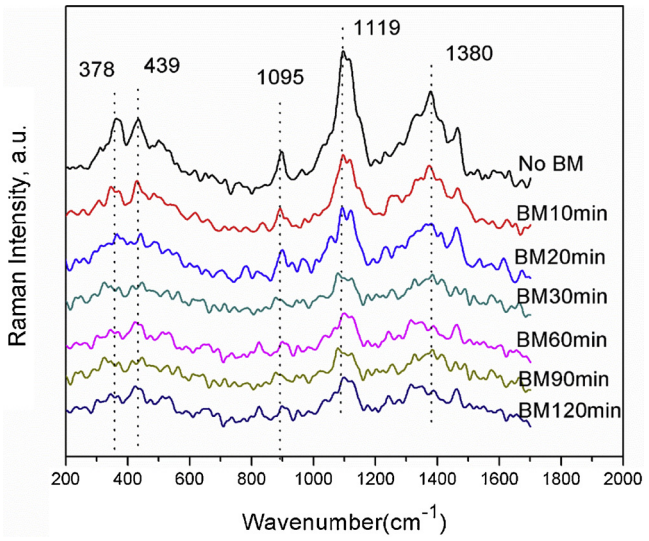

Fig. 9. FT-Raman curves for varied time ball milling cellulose particles.

3.9. Thermal stability

The thermal stability of the milled cellulose samples was shown in Fig. 10. From the TGA and DTG curves, the raw material exhibited a higher decomposition temperature than that of the milled samples. In addition, the thermal decomposition temperature continues to decrease as the milling time increases. As explained above, when cellulose pulp fibers were milled into small particles, the cellulose chains were depolymerized and amorphized, thereby increasing entropy in the system. The increased entropy then led to a decrease in the initial decomposition temperature of the milled samples. As demonstrated in the DTG curves, the degradation temperature for the 10 min sample decreased significantly compared with that of the raw material, implying the destruction of the inter and intra bonds in the cellulose mainly occurred in the early milling stage.

3.10. Surface area & energy consumption

One of the most significant advantages of particle size reduction is the increase of the specific surface area, which promotes the accessibility of contact reaction activity. The following Fig. 11 summarized the *SSA* changes upon ball milling. There is no doubt that the raw pulp fiber has the smallest *SSA*, with a value of 27.8 m^2/g. After 10 min of ball milling, the short fiber's surface area increased to 48.3 m^2/g. Then ellipsoid particles began forming at 20 min of ball milling and the *SSA* increased to 61.6 m^2/g. As the milling time further increases, large particles split into small ones and generated more new surfaces. However, after 40 min of ball milling, the increased rate of forming new *SSA* per unit milling time began to slow. For ball milling times of 90 min and 120 min, there is little improvement of the *SSA*, which has reached a plateau. This result agrees with the particle size and distribution analysis mentioned above.

During the particle refinement process, the quantitative measurement of energetics and energy efficiency has attracted much attention, especially in industry. Rittinger's law states that the specific energy consumption is proportional to the newly generated surface, which is represented by the change in the particle diameters (Fuerstenau and Abouzeid, 2002). Here in this study, the specific energy consumption (*SEC*), calculated from the energy consumed divided by the increase of the *SSA* during a specific period of milling, were used to determine the energy needed for generating a new unit of surface area. As shown in

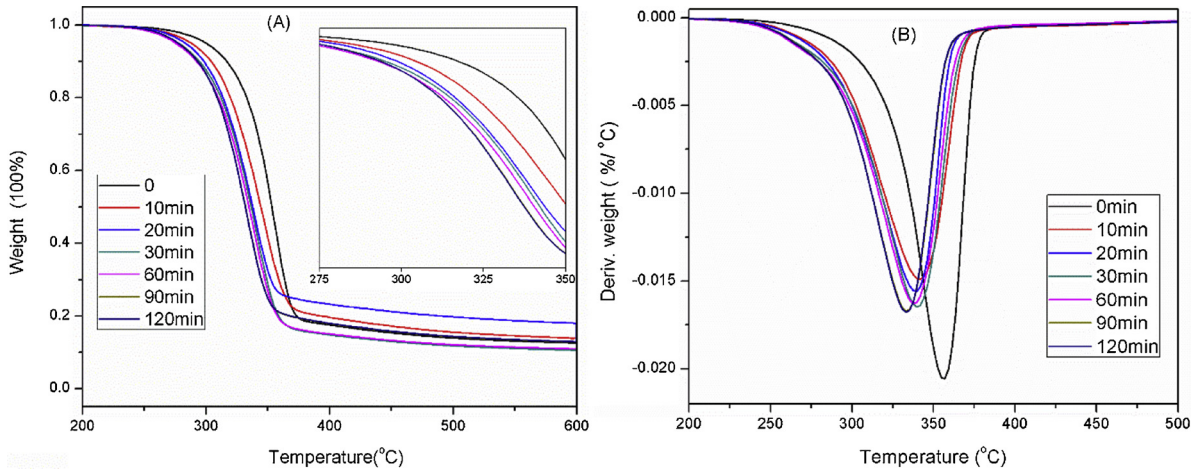

Fig. 10. TGA (A) & DTG(B) curves for different ball milled cellulose samples.

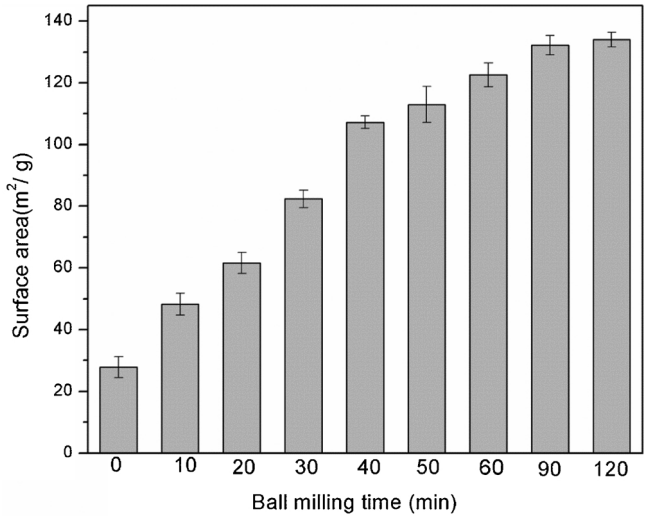

Fig. 11. Specific surface area for pulp fiber and different time ball milled cellulose particles.

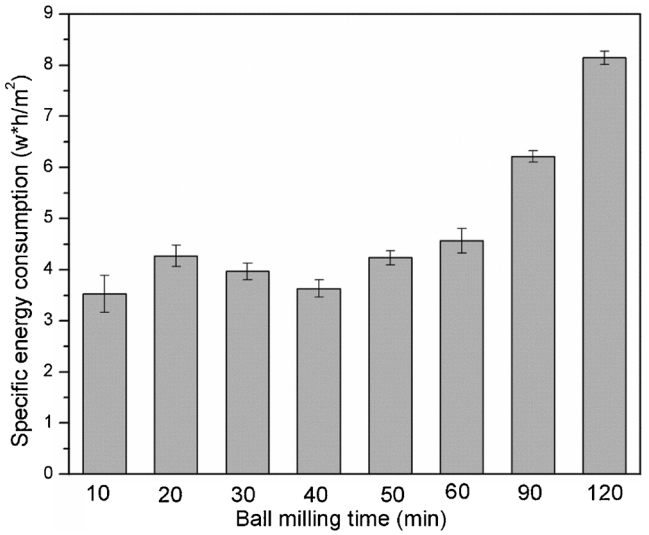

Fig. 12. Specific energy consumption for different time ball milled samples.

Fig. 12, at an early milling stage, the *SEC* is low, but after ball milling for 50 min, the *SEC* increases significantly. The fracture controlling new surface area production is driven by the energy to propagate cracks in the cellulose fiber. This process requires higher energy input than the interfacial energy of the pulp fiber (Griffith, 1920). Theoretically, larger energy consumption would achieve better grinding results. In this case, the energy consumption corresponds to the operating time, the longer the machine runs, the more energies it consumed. However, the specific surface area of the milling samples increased rapidly during the early milling stage but remains unchanged after a certain milling period, so the energy consumption efficiency for long milling times decreased. During long milling times, most of the energy was lost in the form of heat caused by invalid collisions.

4. Conclusions

The assessment of processing parameters ball milling of wood pulp fibers was studied. Ball milling was shown to be an effective grinding approach to prepare micronized cellulose particles. Ball mill time, rotational speed, charge ratio, milling ball diameter, and initial moisture content of pulp fiber have a great influence on the final particle size and distribution. Comminution with ball milling prepares cellulose particles with low aspect ratios, ellipsoid shaped, and high specific surface area. The preferred operating parameters for effective fiber comminution include: ball mill time of 30 ~ 40 min, ball to cellulose mass ratio of 40 ~ 60, rotational speed at ca. 620 rpm, a large ball: small ball mass ratio of 1: 2, and a low fiber moisture content (i.e. less than 3%).

In addition, the milling destroyed the highly ordered crystal structure of cellulose, decreased the degree of crystallinity, as well as the thermal stability of the resulting cellulose powders. This study provides valuable guidance for optimized milling experiment designation with better yields and lower energy consumptions, which could be beneficial for further cellulosic materials comminution or activation in laboratory or scale up applications.

Acknowledgements

The authors would like to thank the louisiana pacific quasi-endowment, and China Postdoctoral Science Foundation Grant (2019M652504) for the financial support.

References

Alves, A.P.P., de Oliveira, L.P., Castro, A.A., Neumann, R., de Oliveira, L.F., Edwards, H.G., Sant'Ana, A.C., 2016. The structure of different cellulosic fibres characterized by Raman spectroscopy. Vib. Spectrosc. 86, 324–330.

Ashori, A., 2008. Wood–plastic composites as promising green-composites for automotive

industries!. Bioresour. Technol. 99, 4661–4667.
Austin, L.G., Shoji, K., Luckie, P.T., 1976. The effect of ball size on mill performance. Powder Technol. 14, 71–79.
Balat, M., 2011. Production of bioethanol from lignocellulosic materials via the biochemical pathway: a review. Energy Convers. Manage. 52, 858–875.
Bhatnagar, A., Sain, M., 2005. Processing of cellulose nanofiber-reinforced composites. J. Reinf. Plast. Compos. 24, 1259–1268.
Bon-Jae, G., Wolcott, M.P., Ganjyal, G.M., 2019. Pretreatment with lower feed moisture and lower extrusion temperatures aids in the increase in the fermentable sugar yields from fine-milled Douglas-fir. Bioresour. Technol.
Cellulose, I., 2010. Dordrecht, Netherlands. In: In: Agarwal, U.P., Reiner, R.S., Ralph, S.A.C. (Eds.), Crystallinity Determination Using FT-Raman Spectroscopy: Univariate and Multivariate Methods 17. pp. 721–733.
Edgar, K.J., Buchanan, C.M., Debenham, J.S., Rundquist, P.A., Seiler, B.D., Shelton, M.C., Tindall, D., 2001. Advances in cellulose ester performance and application. Prog. Polym. Sci. 26, 1605–1688.
Edwards, H., Farwell, D., Webster, D., 1997. FT Raman microscopy of untreated natural plant fibres. Spectrochim. Acta A 53, 2383–2392.
Fidale, L.C., Ruiz, N., Heinze, T., Seoud, O.A.E., 2008. Cellulose swelling by aprotic and protic solvents: what are the similarities and differences? Macromol. Chem. Phys. 209, 1240–1254.
Fuerstenau, D., Abouzeid, A.-Z., 2002. The energy efficiency of ball milling in comminution. Int. J. Miner. Process. 67, 161–185.
Goodrich, J.D., Winter, W.T., 2007. α-Chitin nanocrystals prepared from shrimp shells and their specific surface area measurement. Biomacromolecules 8, 252–257.
Griffith, A., 1920. The phenomena of flow and rupture in solids. Phil. Trans. Roy. Soc. Lond. Ser. A 221, 163–198.
Hess, K., Kiessig, H., Gundermann, J., 1941. Röntgenographische und elektronenmikroskopische Untersuchungen der Vorgänge beim Vermahlen von Cellulose. Z. Phys. Chem. B 49, 64–82.
Hult, E.-L., Larsson, P., Iversen, T., 2001. Cellulose fibril aggregation—an inherent property of kraft pulps. Polymer 42, 3309–3314.
Inglesby, M., Zeronian, S., 2002. Direct dyes as molecular sensors to characterize cellulose substrates. Cellulose 9, 19–29.
Isogai, A., Usuda, M., Kato, T., Uryu, T., Atalla, R.H., 1989. Solid-state CP/MAS carbon-13 NMR study of cellulose polymorphs. Macromolecules 22, 3168–3172.
Jiang, J., Wang, J., Zhang, X., Wolcott, M., 2017. Microstructure change in wood cell wall fracture from mechanical pretreatment and its influence on enzymatic hydrolysis. Ind. Crop. Prod. 97, 498–508.
Kennedy, J.F., Phillips, G., Wedlock, D., Williams, P., 1985. Cellulose and its Derivatives: Chemistry, Biochemistry and Applications. Horwood.
Klemm, D., Philipp, B., Heinze, T., Heinze, U., Wagenknecht, W., 2004. General Considerations on Structure and Reactivity of Cellulose: Section 2.1–2.1. 4. Wiley Online Library.
Klemm, D., Schumann, D., Kramer, F., Heßler, N., Hornung, M., Schmauder, H.-P., Marsch, S., 2006. Nanocelluloses as Innovative Polymers in Research and Application, Polysaccharides Ii. Springer, pp. 49–96.
Ling, Z., Wang, T., Makarem, M., Cintrón, M.S., Cheng, H.N., Kang, X., Bacher, M., Potthast, A., Rosenau, T., King, H., 2019. Effects of ball milling on the structure of cotton cellulose. Cellulose 1–24.
Liu, Y., Wang, J., Wolcott, M.P., 2016. Assessing the specific energy consumption and physical properties of comminuted Douglas-fir chips for bioconversion. Ind. Crop. Prod. 94, 394–400.
Segal, L., Creely, J., Martin Jr., A., Conrad, C., 1959. An empirical method for estimating the degree of crystallinity of native cellulose using the X-ray diffractometer. Text. Res. J. 29, 786–794.
Siró, I., Plackett, D., 2010. Microfibrillated cellulose and new nanocomposite materials: a review. Cellulose 17, 459–494.
Stone, J., Scallan, A., 1968. A structural model for the cell wall of water-swollen wood pulp fibres based on their accessibility to macromolecules. Cellul. Chem. Technol. 2, 343–358.
Suryanarayana, C., 2001. Mechanical alloying and milling. Prog. Mater. Sci. 46, 1–184.
Thuresson, K., Lindman, B., Nyström, B., 1997. Effect of hydrophobic modification of a nonionic cellulose derivative on the interaction with surfactants. Rheol. J. Phys. Chem. B 101, 6450–6459.
Wiman, M., Dienes, D., Hansen, M.A., van der Meulen, T., Zacchi, G., Lidén, G., 2012. Cellulose accessibility determines the rate of enzymatic hydrolysis of steam-pretreated spruce. Bioresour. Technol. 126, 208–215.
Wu, Q., Henriksson, M., Liu, X., Berglund, L.A., 2007. A high strength nanocomposite based on microcrystalline cellulose and polyurethane. Biomacromolecules 8, 3687–3692.